# Ice core reconstruction of sea ice change in the Amundsen-Ross Seas since 1702 A.D.

**Elizabeth R. Thomas[1] and Nerilie J. Abram[2]**

[1]British Antarctic Survey, Cambridge, UK, [2]Research School of Earth Sciences, The Australian National University, Canberra, ACT, Australia

**Abstract** Antarctic sea ice has been increasing in recent decades, but with strong regional differences in the expression of sea ice change. Declining sea ice in the Bellingshausen Sea since 1979 (the satellite era) has been linked to the observed warming on the Antarctic Peninsula, while the Ross Sea sector has seen a marked increase in sea ice during this period. Here we present a 308 year record of methansulphonic acid from coastal West Antarctica, representing sea ice conditions in the Amundsen-Ross Sea. We demonstrate that the recent increase in sea ice in this region is part of a longer trend, with an estimated ~1° northward expansion in winter sea ice extent (SIE) during the twentieth century and a total expansion of ~1.3° since 1702. The greatest reconstructed SIE occurred during the mid-1990s, with five of the past 30 years considered exceptional in the context of the past three centuries.

## 1. Introduction

Sea ice plays an important role in modulating Antarctic climate. It is a potential major source of dimethylsulphide (DMS) [*Trevena and Jones*, 2006] (a climate-cooling gas), alters the albedo of the Earth's surface, and is thought to modulate the physical and biological processes that can draw down $CO_2$ from the atmosphere [*Nomura et al.*, 2013]. The total Antarctic sea ice cover has been steadily increasing since systematic satellite observations began in the late 1970s [*Zwally et al.*, 2002; *Turner et al.*, 2009], in contrast to the rapid decline in Arctic sea ice during this period. At a regional scale, Antarctic sea ice trends are more variable; the Weddell Sea and the Ross Sea sectors have shown marked increases in sea ice extent (SIE) [*Cavalieri and Parkinson*, 2008], while the Bellingshausen Sea has seen a marked reduction.

Observations of Antarctic sea ice conditions are limited to the satellite era making it hard to assess the significance of recent regional-scale trends. The chemistry of Antarctic ice cores provides an alternative way to reconstruct past sea ice changes on a range of time scales [*Curran et al.*, 2003; *Wolff et al.*, 2003; *Dixon et al.*, 2005; *Abram et al.*, 2013]. Methane sulphonic acid (MSA) in Antarctic ice cores comes from the atmospheric oxidation of dimethylsulphide (DMS), derived from phytoplankton productivity linked to the sea ice conditions around Antarctica [*Welch et al.*, 1993; *Curran and Jones*, 2000]. In addition to DMS production within the sea ice zone, atmospheric circulation, transport distance and direction, and oxidation processes all influence the concentration of MSA delivered to an ice core site [*Abram et al.*, 2007; *Becagli et al.*, 2009; *Fundel et al.*, 2006; *Preunkert et al.*, 2008]. Biological production of DMS over the Southern Ocean is the only source of MSA in Antarctica, although a recent study using a chemical transport model concluded that only a small fraction of sulphur emissions in the sea ice zone are deposited over the Antarctic continent [*Hezel et al.*, 2011].

A review of sea ice proxies [*Abram et al.*, 2013] demonstrated both positive and negative relationships exist between MSA and SIE from Antarctic ice cores. MSA from the Law Dome ice core was used to reconstruct SIE in the western Pacific (80°E to 140°E) [*Curran et al.*, 2003], and MSA from a stack of ice cores from the western Antarctic Peninsula have been related to SIE in the Bellingshausen-Amundsen Sea [*Abram et al.*, 2010]. At these sites MSA concentrations increase with increasing winter SIE. In contrast, MSA records from the Ross and Amundsen Sea coasts have been linked to summer productivity within the sea ice zone. At Mount Erebus Saddle and Whitehall Glacier, near the southwestern Ross Sea, MSA reflects the presence of nearby open water within the Ross Sea polynya [*Rhodes et al.*, 2009, 2012; *Sinclair et al.*, 2014], while in West Antarctica elevated MSA from a coastal ice core coincides with increased open water within the Pine Island Bay and Amundsen Sea polynyas [*Criscitiello et al.*, 2013]. The varying MSA-sea ice relationships observed in Antarctic ice cores highlight the need for careful site assessments [*Abram et al.*, 2013].

In this paper we assess the suitability of MSA from the Ferringo ice core, from the Bryan Coast of West Antarctica, as a proxy for past sea ice conditions. We establish the physical mechanisms that transport MSA to the ice core site and reveal a positive relationship with winter SIE in the Amundsen and Ross Sea. We use this relationship to estimate the magnitude and significance of past sea ice trends and variability in this region since 1702.

## 2. Method and Data

The 136 m Ferrigno ice core was drilled on the ice divide between the Ferrigno and Pine Island Glaciers in Ellsworth Land, West Antarctica (74.57°S, 86.90°W, 1354 m above sea level). Discrete samples were cut at 5 cm resolution, corresponding to approximately 8 samples per year, and analyzed in a class-100 clean laboratory using a reagent free Dionex IC-2500 anion system with a 4 mm column and a flow rate of 0.5 mL/min. Samples were analyzed over a period of 6 months (within 16 months of drilling), thus potential MSA loss in storage [*Abram et al.*, 2008] is expected to be negligible. There is evidence of MSA migration with depth, shifting from a summer to winter peak below 25 m (Figure S1 in the supporting information) as observed previously [*Pasteur and Mulvaney*, 2000]; however, annual averages were calculated using the seasonal cycle in MSA (preserved for the full length of the core) and thus unbiased by migration. The MSA peak remains within the non-sea-salt sulphate-defined layer, with little evidence for MSA diffusion or loss in the firn (Figure S1). MSA years are calculated as approximately June–July to capture the full spring-summer peak. Eight major volcanic eruptions are identified in the sulphate record and match the annual layer counted ages to within ±1 year. The estimated dating error for 2010–1810 is ±3 months; the estimated error for 1810–1702 is ±1 year [*Thomas et al.*, 2013, 2015]. MSA concentration is converted to flux by multiplying with the annual water-equivalent accumulation, corrected for thinning assuming a vertical strain rate and an ice sheet frozen to the bed [*Thomas et al.*, 2015].

We use two measures of sea ice conditions in this study. Bootstrap Sea Ice Concentrations (SIC) from Nimbus-7 scanning multichannel microwave radiometer and Defense Meteorological Satellite Program Special Sensor Microwave Imager-Special Sensor Microwave Imager/Sounder, available from the National Snow and Ice Data Centre (NSIDC) from 1979 onward [*Comiso et al.*, 2000, 2015], calculated as the percentage of ice cover within a 25 $km^2$ data cell. SIC data are used for spatial correlations (Figure 1). A separate winter SIE record was used to produce the SIE reconstructions in this study, based on the gridded passive microwave estimates of mean sea ice concentration from NSIDC ([*Cavalieri and Parkinson*, 2008; *Meier et al.*, 2006] updated quarterly). Winter SIE is calculated as the northernmost latitude where sea ice concentration is 15% or greater, between 1 July and 1 June each year, available in 1° longitude sectors from 1979 to 2007 [*Raymond*, 2009, 2014]. Chlorophyll *a* concentrations are from Goddard Earth Sciences-Data and Information Services Center Interactive Online Visualization ANd aNalysis Infrastructure, part of NASA's Goddard Earth Sciences Data and Information Services Center. The meteorological data come from the European Centre for Medium-Range Weather Forecasts ERA-interim analysis (1979–2010) [*Dee et al.*, 2011].

A SIE reconstruction based on ice core MSA flux and winter SIE was calculated using a geometric mean regression technique [*Smith*, 2009; *Abram et al.*, 2010], allowing for error in both the MSA record and the satellite-derived winter SIE data. All correlations are carried out using detrended data with the significance levels for Pearson's correlation calculated using the two-tailed *t* test and account for autocorrelation.

## 3. Results and Discussion

### 3.1. Assessing the Sea Ice Proxy

Annual average MSA concentration in the Ferrigno ice core is significantly and positively correlated with annual average SIC in the Amundsen and Ross Seas (hereafter referred to as Amundsen-Ross) (Figure 1). The correlations are stronger when converting concentration to flux, which takes account of the amount of snowfall each year. Snow accumulation should have little effect on the concentration of wet deposited ions, suggesting possible scavenging of MSA by other particles (dust or sea salts) resulting in dry deposition. Alternatively, the enhanced correlations may reflect the close relationship between sea ice and snow accumulation, both of which are driven by atmospheric circulation and winds in this region [*Thomas et al.*, 2015; *Holland and Kwok*, 2012]. The spatial correlations and trends are very similar when using either concentration or flux, but MSA flux (hereafter MSA) was used for all reported correlations and trends given the improved statistical significance.
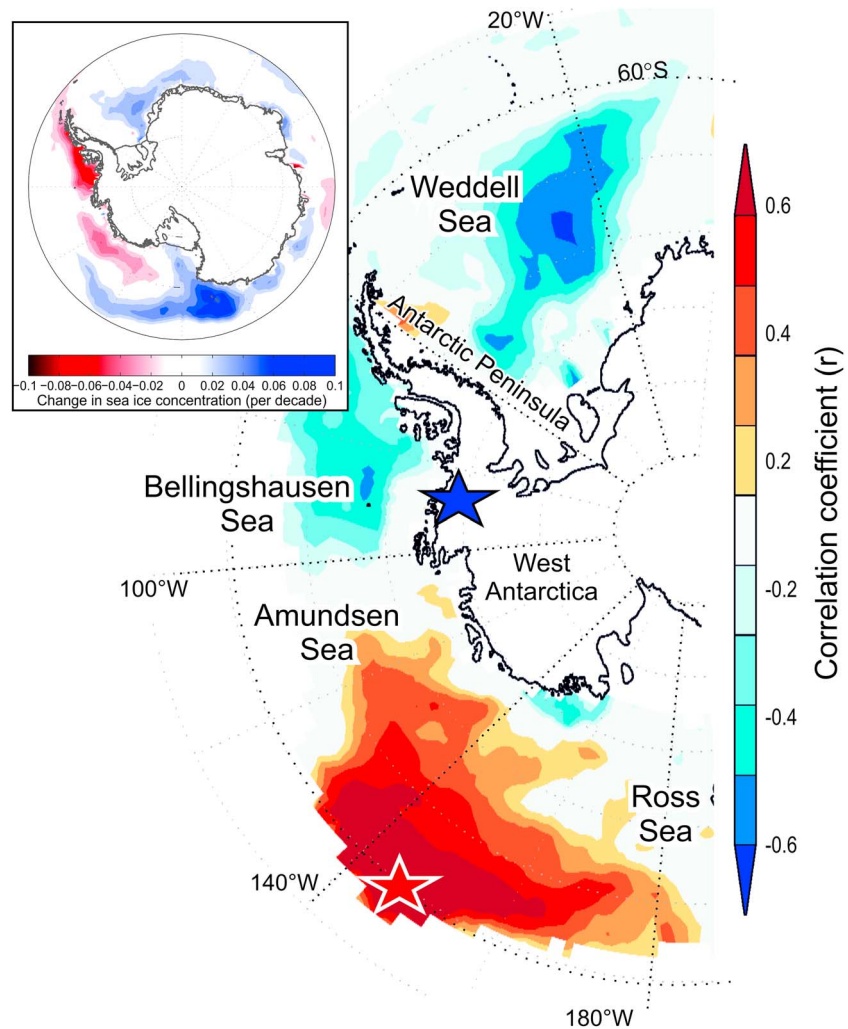
**Figure 1.** (a) Spatial correlation of annual average MSA with annual average sea ice concentration (SIC) (1979–2009) from bootstrap analysis. The darker shading represents correlations exceeding $p > 0.05$. The blue star indicates ice core location; the red star indicates location of greatest correlation with winter SIE (red curve Figure 3a). Inset trends in Antarctic sea ice concentration (1979s2010) from bootstrap analysis.

The greatest correlation between annual average MSA and gridded SIC across the Southern Ocean, occurs in the sector spanning ~160°W and 120°W ($p < 0.01$; 1981–2010), with maximum correlations at 146°W ($r > 0.7$) close to the ice edge (~62°S) (Figure 1). Correlating MSA with seasonal SIC data shows that the greatest correlations occur during the months of sea ice breakup and enhanced marine productivity (September to January).

A similar significant positive correlation is found between MSA and the satellite-derived winter (August–October) SIE in the Amundsen-Ross Sea. The area of significant correlations ($p < 0.01$) extends between 179°W and 129°W, with maximum values observed at 146°W ($r = 0.64$). The positive correlation between MSA and sea ice conditions in the Amundsen-Ross Sea is consistent with the relationships used for previous quantified sea ice reconstructions [*Curran et al.*, 2003; *Abram et al.*, 2010].

The spatial correlation plots of MSA with SIC (Figure 1) reveal a region of statistically significant ($p < 0.01$) negative correlations in the Weddell Sea sector and smaller negative correlations in the Bellingshausen Sea. This reflects the well-known dipole pattern of opposed sea ice variability and trends in the Amundsen-Ross Sea compared with sea ice in the Bellingshausen and Weddell Seas [*Turner et al.*, 2009].

To further test the relationship between MSA and sea ice we utilize the satellite-derived chlorophyll $a$ concentrations. Chlorophyll is a pigment predominant in all oxygen-evolving photosynthetic organisms such as red and green algae. Elevated chlorophyll $a$ concentrations around Antarctica are linked to increased biogenic
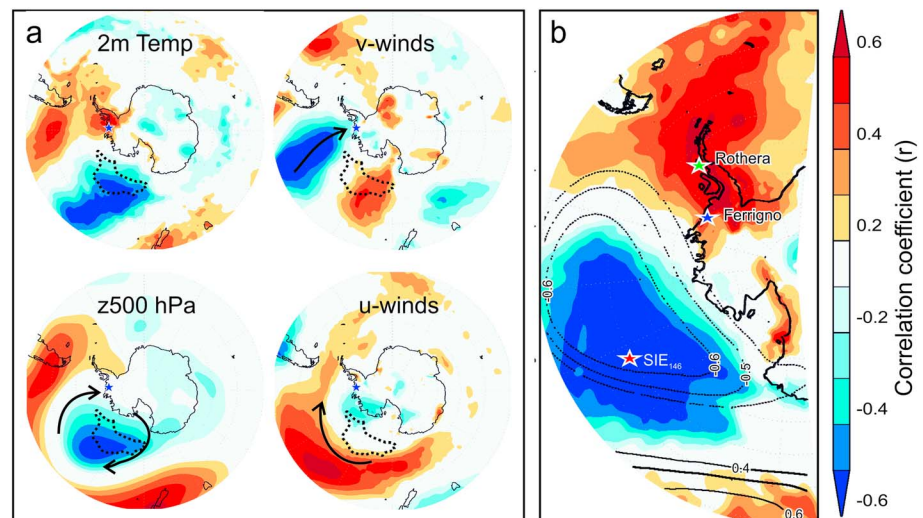
**Figure 2.** (a) Spatial correlation plots of annual average MSA with annual average 2 m temperature, 2 m zonal ($u$)-winds, 500 hPa geopotential height, and 2 m meridional ($v$)-winds from ERA-interim 1979–2009. The dashed area represents zone of significant positive correlations between MSA and SIC (Figure 1), the arrows indicate wind direction, and the star marks ice core location. (b) Spatial correlation plot of winter SIE [*Raymond*, 2009, 2014] at 146°W (SIE$_{146}$) with 2 m temperatures (shading) and 500 hPa geopotential heights (contours) from ERA-interim (1979–2007). The stars indicate locations of SIE$_{146}$, Ferrigno ice core, and Rothera station (timeseries shown in Figure 3). The darker shading represents correlations exceeding $p > 0.05$.

activity and hence increased MSA production. MSA is positively correlated with January (the month of greatest biological production) chlorophyll $a$ concentrations (1998–2007) in the Amundsen-Ross Sea. The region of greatest correlation ($r > 0.5$) corresponds to the ice edge (60–65°S) between 150°W and 140°W, coincident with the area of greatest correlation between MSA, SIC, and SIE.

### 3.2. Transport Pathways for MSA

We now explore the processes driving the observed positive correlation between Ferrigno MSA and sea ice in the Amundsen-Ross Sea. Back trajectory analysis has demonstrated that 48% of all air masses reaching the Ferrigno site originate (5 days before reaching the site) from the Amundsen-Bellingshausen Sea [*Thomas and Bracegirdle*, 2015]. The westward extent of 5 day trajectories from winter (the season of greatest sea ice) to spring (the season of greatest sea ice retreat and MSA production) is between 150 and 130°W, coincident with the area of greatest correlation between ice core MSA and SIC, SIE, and chlorophyll $a$.

MSA is significantly correlated with 500 hPa geopotential heights in the Amundsen-Ross Sea (Figure 2a). The region of statistically significant ($p < 0.01$) negative correlation corresponds to the Amundsen Sea Low (ASL) [*Baines and Fraedrich*, 1989], a quasi-stationary area of climatological low pressure driven by large-scale atmospheric variability, shown to influence climate in West Antarctica [*Hosking et al.*, 2013]. A persistent and deep ASL enhances southerly (offshore) winds over the southern Ross Sea (Figure 2b) cooling surface air temperatures, opening up polynas and creating a region of strong sea ice production. This is accompanied by strengthened westerly winds over the southern South Pacific (Figure 2c) and enhanced northerly flow over the Bellingshausen Sea (Figure 2b). The northerly winds across the Bellingshausen Sea bring warm air to the region resulting in increased surface temperatures (Figure 2d) and snowfall over the southwestern Antarctic Peninsula [*Thomas et al.*, 2008] and Ellsworth Land [*Thomas et al.*, 2013, 2015].

Wind-driven changes in ice advection are the dominant driver of sea ice-concentration trends around West Antarctica [*Holland and Kwok*, 2012]. As demonstrated above, the mechanism for enhanced deposition of MSA at Ferrigno is intrinsically linked with enhanced sea ice production in the Amundsen-Ross Sea. Thus, not only is there a clear mechanism for MSA to be transported from the ice edge to the Ferrigno site, but the factors governing this transport (local wind conditions) are also positively related to the sea ice concentration itself, making this a particularly valuable region for sea ice reconstruction.
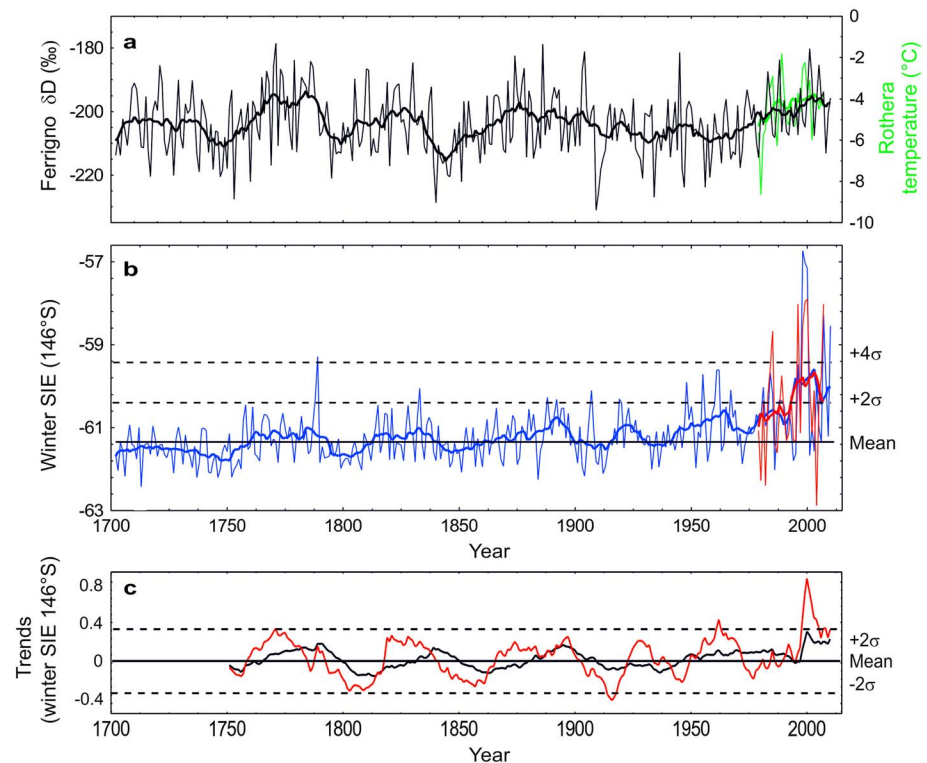
**Figure 3.** (a) Ferrigno stable isotope (δD, black) and Rothera temperature (green) records. (b) Winter SIE reconstruction (blue) for the Amundsen-Ross Sea and satellite derived winter SIE (red) at 146°W [*Raymond*, 2009, 2014] (red star Figure 1) as annual averages (thin lines) and running decadal means (thick lines). Running (c) 30 year (red) and (d) 50 year (black) slopes (degree of latitude per decade). The horizontal dashed lines (Figures 3b and 3d) indicate standard deviation (σ) ranges around the baseline mean (1702–1899, solid horizontal line).

### 3.3. Relationship Between Sea Ice and Temperature

Reductions in sea ice extent in the Bellingshausen Sea have been related to the warming trends observed in West Antarctic climate reconstructions [*Steig et al.*, 2009; *Küttel et al.*, 2012] and may account for ~80% of the spring warming on the Antarctica Peninsula and ~20–30% of the inland warming in West Antarctica [*Schneider et al.*, 2012]. The relationship between winter SIE and surface air temperature is demonstrated when correlating observed winter SIE from 146°W (the area of greatest significance with MSA) with 2 m temperatures from ERA-interim (Figure 2b). Enhanced southerly winds, resulting in cooling and increased SIE in the Amundsen-Ross Sea sector, are innately linked to the increased northerly transport of warm air over the Antarctic Peninsula and reduced SIE in the Bellingshausen Sea (Figure 2).

The warming since the 1950s, observed in instrumental (such as Rothera (green) Figure 3a) and proxy records [*Thomas et al.*, 2009, 2013], is coincident with increasing trends in MSA. This relationship between regional sea ice conditions and surface temperature is maintained back to 1702, as demonstrated by the positive correlations between MSA and stable isotopes (δD) throughout the Ferrigno ice core record (decadal $r = 0.66$, $p > 0.01$; Figure 3a). Confirming that sea ice variability in the Amundsen-Ross Sea has been dynamically connected to a large portion of the decadal climate variability at this site over the past three centuries.

### 3.4. Reconstructed Sea Ice Changes

We use the MSA record to produce a quantified reconstruction of Amundsen-Ross sea ice change since 1702. Satellite observations of winter SIE at 146°W (the latitude of maximum correlation) was calculated using geometric mean regression of MSA. Winter SIE is our instrumental target to allow comparison with previous reconstructions for other Antarctic regions [*Curran et al.*, 2003; *Abram et al.*, 2010].

Our reconstruction reveals an estimated twentieth century expansion in winter SIE of ~1.0°, based on the difference between the average at the start (1900–1919) and end (1981–1999) of the century. The twentieth century expansion of ~0.12° ± 0.02° per decade (based on linear trends) followed a more gradual positive
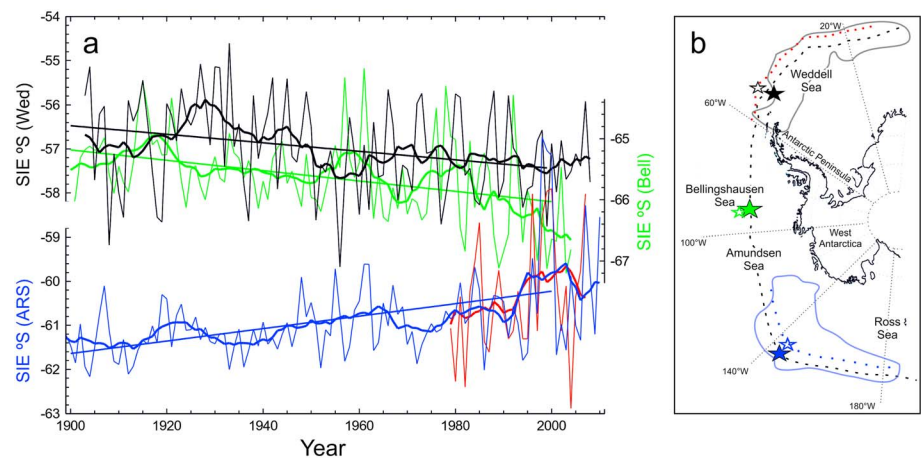
**Figure 4.** (a) Reconstructed twentieth century winter SIE from Ferrigno MSA (blue), Antarctic Peninsula stacked MSA [*Abram et al.*, 2010] (green), and South Orkney fast ice (black, duration in days regressed onto average winter SIE between 15 and 50°W). Winter SIE at 146°W from satellite data are also shown [*Raymond*, 2009, 2014] (red). Time series plotted as annual averages (thin) and decadal running means (thick). (b) Location of SIE reconstructions (full stars) plotted on current average winter SIE [*Raymond*, 2009, 2014] (1979–2007, black dashed line) and estimated location of average winter SIE during 1902–1931 (open stars and dotted lines indicate expansion (red) and retreat (blue)). Area of significance between reconstruction and SIC for South Orkney (grey outline) and Ferrigno MSA (blue line).

trend (0.03° per decade) during the previous two centuries, resulting in a total northward expansion of ~1.3° since 1702. Winter SIE in the reconstruction reached its highest levels in the mid-1990s (1994–2004), when the running decadal mean exceeds 3 standard deviations above the record baseline (1702–1899). At an annual scale, five of the most recent 30 years exceed 4 standard deviations above the reconstruction baseline mean (1702–1899) and may be considered exceptional in the context of the past three centuries. Prior to 1979 this threshold is only exceeded once (1789), indicating that the frequency with which these large SIE years occur has increased in recent decades. The greatest SIE expansion occurred in 1998/1999, coincident with exceptionally strong El Niño–Southern Oscillation (ENSO), an equatorward shift in the circumpolar wester-ly winds [*Hanna*, 2001] and the warmest year in the Gomez isotope record from the southwest Antarctic Peninsula [*Thomas et al.*, 2009]. The relationship between reconstructed SIE and the Southern Oscillation Index, a commonly used measure of the strength and phase of ENSO, is positive from 1979 onward, but as has been demonstrated for stable isotopes and snow accumulation in this region, this relationship is not stable further back in time [*Thomas et al.*, 2008, 2013, 2015].

When viewed over the last three centuries it becomes evident that substantial multidecadal variability char-acterizes sea ice dynamics in the Amundsen-Ross Sea, but the largest 30 and 50 year trends since 1702 (Figure 3c) occurred at the end of the twentieth century (1970–2000 and 1950–2000, respectively). Interannual to decadal SIE variability in the most recent decades appears to be higher than at any point in the 308 year record, which may be linked to reports of higher cyclone counts in this region [*Simmonds et al.*, 2003] and is consistent with increased variability in the snow accumulation record [*Thomas et al.*, 2015].

### 3.5. Comparison With Other Reconstructions

The reconstructed SIE in the Amundsen-Ross Sea supports other reconstructions of sea ice and marine produc-tivity further west in the Ross Sea. The MSA record from Mount Erebus saddle [*Rhodes et al.*, 2009, 2012] is signif-icantly negatively correlated with our reconstruction ($r = -0.37$, $p > 0.01$; 1875–2007). The decreasing twentieth century trend in MSA from Mount Erebus, interpreted as reduced productivity and open water, is in agreement with increased SIE (and hence increased SIC) in our reconstruction. The deuterium excess record from the Whitehall Glacier ice core [*Sinclair et al.*, 2014] reveals a rapid change from stable to highly variable sea ice con-ditions in the Ross Sea since the 1950s, with high sea ice area during the 1990's, consistent with our findings.

Looking at the wider Antarctic, studies have revealed twentieth century reductions in SIE in the Indian sector [*Curran et al.*, 2003], the Bellingshausen Sea [*Abram et al.*, 2010], and the Weddell Sea [*Murphy et al.*, 2014; *Abram et al.*, 2010]. This pattern of opposing positive and negative sea ice trends between different regions

is a prominent feature of Antarctic sea ice dynamics during the satellite period. The estimated 0.9° northward expansion of winter SIE (1900-1990) in the Amundsen-Ross Sea is of a similar magnitude to the ~0.7° southward retreat in the Bellingshausen Sea estimated from Antarctic Peninsula ice cores [*Abram et al.*, 2010] and the ~0.5° retreat in winter SIE in the Weddell Sea [*Abram et al.*, 2010] based on the observed fast ice duration at the South Orkney Islands [*Murphy et al.*, 2014] (Figure 4). This suggests that the characteristic dipole pattern of sea ice expansion in the Amundsen-Ross Sea and sea ice retreat in the Bellingshausen and Weddell Seas seen during the post-1979 satellite era (Figure 1 inset) has been a persistent feature of regional sea ice dynamics over at least the full twentieth century.

Increased SIE in the Ross Sea has been linked to the deepening of the ASL, resulting in greater cold airflow off the Ross Ice Shelf [*Turner et al.*, 2009]. At the same time, a deepening trough causes enhanced onshore winds over the Bellingshausen Sea, leading to basal melting of ice shelves [*Pritchard et al.*, 2012], warming surface temperatures [*Thomas et al.*, 2009, 2013; *Steig et al.*, 2009], and a twentieth century increase in snowfall on the Bryan Coast [*Thomas et al.*, 2015]. Pressure in the ASL region during the observational period (1979 onward) is strongly modulated by large-scale modes of climate variability such as the Southern Annular Mode (SAM) [*Turner et al.*, 2009] and ENSO [*Fogt et al.*, 2012]. However, the relationship between our SIE reconstruction and both SAM and ENSO varies through time (as observed for other climate parameters). The strength of the ENSO-related tropical forcing to the ASL region may be dependent on the degree to which these two climate patterns are in phase [*Clem and Fogt*, 2013], explaining the high values in our SIE reconstruction during the 1990s, when both SAM and ENSO were in their positive phases. The positive trend of the SAM, especially during the austral summer, is attributed to Antarctic ozone depletion and greenhouse gas emissions [*Kushner et al.*, 2001; *Arblaster and Meehl*, 2006], while *Turner et al.* [2009] concluded that anthropogenic forcing is primarily responsible for the circulation changes leading to increased SIE in the Ross Sea sector.

## 4. Conclusions

The Ferrigno MSA record is a robust proxy for SIC and winter SIE in the Amundsen-Ross Sea (150°W to 130°W). High MSA (increased SIE) years are associated with a deepening of the low-pressure system in the Amundsen Sea (the ASL) and a regional expansion and intensification of the westerly jet. This mechanism has the dual effect of both increasing sea ice concentration (and hence MSA production) in the Amundsen-Ross Sea while simultaneously enhancing transport of MSA from the ice edge to the ice core site. The link between MSA and biological activity at the ice edge is further confirmed using observations of chlorophyll concentrations.

SIE in the Amundsen-Ross Sea explains a large amount of the decadal variability in surface temperatures in the western Antarctic Peninsula and coastal Ellsworth Land over the past 300 years, via the influence of low-pressure anomalies in the Amundsen Sea. Enhanced southerly flow that increases SIE in the Ross Sea is intrinsically linked to the increased northerly flow in the Bellingshausen Sea that draws warm maritime air to the southwestern Antarctic Peninsula.

The Amundsen-Ross sea ice reconstruction reveals an estimated ~1° northward expansion of winter SIE during the twentieth century and an overall expansion of ~1.3° since 1702. In contrast, reconstructions in the Bellingshausen and Weddell Seas (and the Indian sector) reveal a twentieth century decline, confirming that a dipole pattern in sea ice trends has been a persistent feature of regional ice dynamics for at least the last 100 years. The largest 50 and 30 year trends occurred at the end of the twentieth century, with the highest absolute values observed during the mid-1990s. This suggests that the long-term trends in sea ice in the Amundsen-Ross Sea are now highly unusual in the context of the past three centuries.

## References

Abram, N. J., R. Mulvaney, E. W. Wolff, and M. Mudelsee (2007), Ice core records as sea ice proxies: An evaluation from the Weddell Sea region of Antarctica, *J. Geophys. Res.*, *112*, D15101, doi:10.1029/2006JD008139.
Abram, N. J., M. A. J. Curran, R. Mulvaney, and T. Vance (2008), The preservation of methanesulphonic acid in frozen ice-core samples, *J. Glaciol.*, *54*(187), 680–684.
Abram, N. J., E. R. Thomas, J. R. McConnell, R. Mulvaney, T. J. Bracegirdle, L. C. Sime, and A. J. Aristarain (2010), Ice core evidence for a 20th century decline of sea ice in the Bellingshausen Sea, Antarctica, *J. Geophys. Res.*, *115*, D23101, doi:10.1029/2010JD014644.
Abram, N. J., E. W. Wolff, and M. A. J. Curran (2013), A review of sea ice proxy information from polar ice cores, *Quat. Sci. Rev.*, *79*, 168–183.
Arblaster, J. M., and G. A. Meehl (2006), Contributions of external forcings to southern annular mode trends, *J. Clim.*, *19*(12), 2896–2905.
Baines, P. G., and K. Fraedrich (1989), Topographic effects on the mean tropospheric flow patterns around Antarctica, *J. Atmos. Sci.*, *46*, 3401–3415.

Becagli, S., et al. (2009), Methanesulphonic acid (MSA) stratigraphy from a Talos Dome ice core as a tool in depicting sea ice changes and southern atmospheric circulation over the previous 140 years, *Atmos. Environ.*, *43*(5), 1051–1058.

Cavalieri, D. J., and C. L. Parkinson (2008), Antarctic sea ice variability and trends, 1979–2006, *J. Geophys. Res.*, *113*, C07004, doi:10.1029/2007JC004564.

Clem, K. R., and R. L. Fogt (2013), Varying roles of ENSO and SAM on the Antarctic Peninsula climate in austral spring, *J. Geophys. Res. Atmos.*, *118*, 11,481–11,492, doi:10.1002/jgrd.50860.

Comiso, J. C. (2000, 2015), *Bootstrap Sea Ice Concentrations from Nimbus-7 SMMR and DMSP SSM/I-SSMIS, Version 2*, NASA National Snow and Ice Data Center Distributed Active Archive Center, Boulder, Colo.

Criscitiello, A. S., S. B. Das, M. J. Evans, K. E. Frey, H. Conway, I. Joughin, B. Medley, and E. J. Steig (2013), Ice sheet record of recent sea-ice behavior and polynya variability in the Amundsen Sea, West Antarctica, *J. Geophys. Res. Oceans*, *118*, 118–130, doi:10.1029/2012JC008077.

Curran, M. A. J., and G. B. Jones (2000), Dimethyl sulfide in the Southern Ocean: Seasonality and flux, *J. Geophys. Res.*, *105*, 20,451–20,459, doi:10.1029/2000JD900176.

Curran, M. A. J., T. D. van Ommen, V. I. Morgan, K. L. Phillips, and A. S. Palmer (2003), Ice core evidence for Antarctic sea ice decline since the 1950s, *Science*, *302*, 1203–1206.

Dee, D. P., et al. (2011), The ERA-Interim reanalysis: Configuration and performance of the data assimilation system, *Q. J. R. Meteorol. Soc.*, *137*(656), 553–597.

Dixon, D. A., P. A. Mayewski, S. Kaspari, K. Kreutz, G. Hamilton, K. Maasch, S. B. Sneed, and M. J. Handley (2005), A 200 year sulfate record from 16 Antarctic ice cores and associations with Southern Ocean sea-ice extent, *Ann. Glaciol.*, *41*, 155–166.

Fogt, R. L., A. J. Wovrosh, R. A. Langen, and I. Simmonds (2012), The characteristic variability and connection to the underlying synoptic activity of the Amundsen-Bellingshausen Sea Low, *J. Geophys. Res.*, *117*, D07111, doi:10.1029/2011JD017337.

Fundel, F., H. Fischer, R. Weller, F. Traufetter, H. Oerter, and H. Miller (2006), Influence of large-scale teleconnection patterns on methane sulfonate ice core records in Dronning Maud Land, *J. Geophys. Res.*, *111*, D04103, doi:10.1029/2005JD005872.

Hanna, E. (2001), Anomalous peak in Antarctic sea-ice area, Winter 1998, coincident with ENSO, *Geophys. Res. Lett.*, *28*(8), 1595–1598, doi:10.1029/2000GL012368.

Hezel, P. J., B. Alexander, C. M. Bitz, E. J. Steig, C. D. Holmes, X. Yang, and J. Sciare (2011), Modeled methanesulfonic acid (MSA) deposition in Antarctica and its relationship to sea ice, *J. Geophys. Res.*, *116*, D23214, doi:10.1029/2011JD016383.

Holland, P. R., and R. Kwok (2012), Wind-driven trends in Antarctic sea-ice drift, *Nat. Geosci.*, *5*(12), 872–875.

Hosking, J. S., A. Orr, G. J. Marshall, J. Turner, and T. Phillips (2013), The influence of the Amundsen–Bellingshausen Seas Low on the climate of West Antarctica and its representation in coupled climate model simulations, *J. Clim.*, *26*(17), 6633–6648.

Kushner, P. J., I. M. Held, and T. L. Delworth (2001), Southern Hemisphere atmospheric circulation response to global warming, *J. Clim.*, *14*(10), 2238–2249.

Küttel, M., E. J. Steig, Q. Ding, A. J. Monaghan, and D. S. Battisti (2012), Seasonal climate information preserved in West Antarctic ice core water isotopes: Relationships to temperature, large-scale circulation, and sea ice, *Clim. Dyn.*, *39*(7), 1841–1857.

Meier, W., F. Fetterer, K. Knowles, M. Savoie, and M. J. Brodzik (2006), Sea ice concentrations from Nimbus-7 SMMR and DMSP SSM/I passive microwave data, in *Digital Media*, National Snow and Ice Data Center, Boulder, Colo.

Murphy, E. J., A. Clarke, N. J. Abram, and J. Turner (2014), Variability of sea-ice in the northern Weddell Sea during the 20th century, *J. Geophys. Res. Oceans*, *119*, 4549–4572, doi:10.1002/2013JC009511.

Nomura, D., M. A. Granskog, P. Assmy, D. Simizu, and G. Hashida (2013), Arctic and Antarctic sea ice acts as a sink for atmospheric CO2 during periods of snowmelt and surface flooding, *J. Geophys. Res. Oceans*, *118*, 6511–6524, doi:10.1002/2013JC009048.

Pasteur, E. C., and R. Mulvaney (2000), Migration of methane sulphonate in Antarctic firn and ice, *J. Geophys. Res.*, *105*(D9), 11,525–11,534, doi:10.1029/2000JD900006.

Preunkert, S., B. Jourdain, M. Legrand, R. Udisti, S. Becagli, and O. Cerri (2008), Seasonality of sulfur species (dimethyl sulfide, sulfate, and methanesulfonate) in Antarctica: Inland versus coastal regions, *J. Geophys. Res.*, *113*, D15302, doi:10.1029/2008JD009937.

Pritchard, H. D., S. R. M. Ligtenberg, H. A. Fricker, D. G. Vaughan, M. R. van den Broeke, and L. Padman (2012), Antarctic ice-sheet loss driven by basal melting of ice shelves, *Nature*, *484*(7395), 502–505.

Raymond, B. (2009, 2014), The maximum extent of sea ice in the southern hemisphere by day and by winter season Australian Antarctic Data Centre. [Available at http://data.aad.gov.au/aadc/metadata/metadata_redirect.cfm?md=/AMD/AU/sea_ice_extent_winter.]

Rhodes, R. H., N. A. N. Bertler, J. A. Baker, S. B. Sneed, H. Oerter, and K. R. Arrigo (2009), Sea ice variability and primary productivity in the Ross Sea, Antarctica, from methylsulphonate snow record, *Geophys. Res. Lett.*, *36*, L10704, doi:10.1029/2009GL037311.

Rhodes, R. H., N. A. N. Bertler, J. A. Baker, H. C. Steen-Larsen, S. B. Sneed, U. Morgenstern, and S. J. Johnsen (2012), Little Ice Age climate and oceanic conditions of the Ross Sea, Antarctica from a coastal ice core record, *Clim. Past*, *8*, 1223–1238.

Schneider, D. P., C. Deser, and Y. Okumura (2012), An assessment and interpretation of the observed warming of West Antarctica in the austral spring, *Clim. Dyn.*, *38*(1), 323–347.

Simmonds, I., K. Keay, and E.-P. Lim (2003), Synoptic activity in the seas around Antarctica, *Mon. Weather Rev.*, *131*, 272–288.

Sinclair, K. E., N. A. N. Bertler, M. M. Bowen, and K. R. Arrigo (2014), Twentieth century sea-ice trends in the Ross Sea from a high-resolution, coastal ice-core record, *Geophys. Res. Lett.*, *41*, 3510–3516, doi:10.1002/2014GL059821.

Smith, R. J. (2009), Use and misuse of the reduced major axis for line-fitting, *Am. J. Phys. Anthropol.*, *140*, 476–486.

Steig, E. J., D. P. Schneider, S. D. Rutherford, M. E. Mann, J. C. Comiso, and D. T. Shindell (2009), Warming of the Antarctic ice-sheet surface since the 1957 International Geophysical Year, *Nature*, *457*, 459–462.

Thomas, E. R., and T. J. Bracegirdle (2015), Precipitation pathways for five new ice core sites in Ellsworth Land, West Antarctica, *Clim. Dyn.*, *44*(7-8), 2067–2078, doi:10.1007/s00382-014-2213-6.

Thomas, E. R., G. J. Marshall, and J. R. McConnell (2008), A doubling in accumulation in the western Antarctic Peninsula since 1850, *Geophys. Res. Lett.*, *35*, L01706, doi:10.1029/02007GL032529.

Thomas, E. R., P. F. Dennis, T. J. Bracegirdle, and C. Franzke (2009), Ice core evidence for significant 100-year regional warming on the Antarctic Peninsula, *Geophys. Res. Lett.*, *36*, L20704, doi:10.1029/2009GL040104.

Thomas, E. R., T. J. Bracegirdle, J. Turner, and E. W. Wolff (2013), A 308 year record of climate variability in West Antarctica, *Geophys. Res. Lett.*, *40*, 5492–5496, doi:10.1002/2013GL057782.

Thomas, E. R., J. S. Hosking, R. R. Tuckwell, R. A. Warren, and E. C. Ludlow (2015), Twentieth century increase in snowfall in coastal West Antarctica, *Geophys. Res. Lett.*, *42*, 9387–9393, doi:10.1002/2015GL065750.

Trevena, A. J., and G. B. Jones (2006), Dimethylsulphide and dimethylsulphoniopropionate in Antarctic sea ice and their release during sea ice melting, *Mar. Chem.*, *98*, 210–222.

Turner, J., J. C. Comiso, G. J. Marshall, T. A. Lachlan-Cope, T. Bracegirdle, T. Maksym, M. P. Meredith, Z. Wang, and A. Orr (2009), Non-annular atmospheric circulation change induced by stratospheric ozone depletion and its role in the recent increase of Antarctic sea ice extent, *Geophys. Res. Lett.*, *36*, L08502, doi:10.1029/2009GL037524.

Welch, K. A., P. A. Mayewski, and S. I. Whitlow (1993), Methansulfonic-acid in coastal Anatrctic snow related to sea-ice extent, *Geophys. Res. Lett.*, *20*, 443–446, doi:10.1029/93GL00499.

Wolff, E. W., Rankin, A. M., and Rothlisberger, R. (2003), An ice core indicator of Antarctic sea ice production?, *Geophys. Res. Lett.*, *30*(22), 2158, doi:10.1029/2003GL018454.

Zwally, H. J., J. C. Comiso, C. L. Parkinson, D. J. Cavalieri, and P. Gloersen (2002), Variability of Antarctic sea ice 1979–1998, *J. Geophys. Res.*, *107*(C5), 3041, doi:10.1029/2000JC000733.